Pergamon

0022–3697(94)E0024–A

J. Phys. Chem. Solids Vol. 55, No. 7, pp. 589–593, 1994

0022-3697/94 $7.00 + 0.00

SOLID STATE NMR STUDY SUPPORTING THE LITHIUM VACANCY DEFECT MODEL IN CONGRUENT LITHIUM NIOBATE

J. BLÜMEL,† E. BORN‡ and TH. METZGER‡

†Anorganisch-chemisches Institut der Technischen Universität München, Lichtenbergstraße 4, 85747 Garching, Germany

‡Lehrstuhl für Angewandte Mineralogie und Geochemie der Technischen Universität München, Lichtenbergstraße 4, 85747 Garching, Germany

(*Received* 12 *November* 1993; *accepted* 1 *March* 1994)

Abstract—^{93}Nb and ^{7}Li wideline- as well as MAS-NMR measurements were performed on powdered and single crystal lithium niobate of defective congruent composition (48.4% Li_2O; 51.6% Nb_2O_5) using a magnetic field strength of 7.05 Tesla with the aim to distinguish between a lithium vacancy defect model (1% of the Nb atoms in a different site) and a niobium vacancy defect model (5% of the Nb atoms in a different site). Although the line width of the ^{7}Li signal of powdered lithium niobate could be reduced to 0.6 kHz by using MAS-NMR with a rotational frequency of 4000 Hz, there was no second ^{7}Li signal apparent, indicating different chemical surroundings for ^{7}Li nuclei caused by the defect structure. The wideline spectra of ^{93}Nb NMR measurements on lithium niobate single crystals in various orientations do not exhibit a second resonance and therefore contradict several earlier ^{93}Nb NMR studies from which a niobium defect model was substantiated. Additionally, earlier NMR measurements could be explained on the basis of the complex ^{93}Nb MAS spectra of powdered material.

Keywords: D. crystal structure, D. defects, D. nuclear magnetic resonance (NMR).

INTRODUCTION

The technical application of congruently grown lithium niobate (LN) single crystals includes the production of surface acoustic wave (SAW) band filters to be integrated in each new TV set; about 250,000 filters are produced daily in one plant. In spite of the high commercial interest in this material, there is still a discussion about the defect model in the congruent non-stoichiometric LN. The ideal structure of LN at room temperature can be described as distorted hexagonal close packing of oxygen atoms forming three different octahedral sites [1]. The smallest octahedral site is occupied by Nb atoms, the octahedron of intermediate size is occupied by Li atoms and the greatest remains unoccupied [2]. Thus, two-thirds of all octahedra are occupied by cations. Along the axis c_{hex} the occupancy of octahedra can be written as {Li o Nb Li o Nb}, where "o" denotes an empty octahedron. Czochralsky grown crystals of congruently melting composition consist of 48.4% Li_2O and 51.6% Nb_2O_5 [3], which differs from the 1:1 ratio of cation concentrations described by the formula $LiNbO_3$ and must therefore have a defect structure. Until 1993, a model was favoured [4] that includes Li substitution by Nb atoms with accompanied Nb vacancies at Nb sites for charge neutrality. This model was initiated by an NMR study [5]. Recent X-ray and neutron scattering studies [6, 7], however, revealed a fully occupied Nb sublattice contradicting the Nb vacancy defect model proposed in Ref. [4]. Thus, the necessity arises to improve several NMR measurements [5, 8–14], some of them supporting the Nb vacancy defect model.

PRESENT STATE OF NON-STOICHIOMETRY DEFECT INTERPRETATION IN LN

The excess of Nb in congruent LN is only expected on Li sites [4, 6, 7, 15]. At the tetrahedral site it cannot be expected [16]. The required local charge neutrality can theoretically be guaranteed either by oxygen deficiency [17], by Li vacancies at Li sites or by Nb vacancies at Nb sites. These defects can be written in the three notations listed in Table 1.

Model 1 can be ruled out by precise measurements of density according to Refs [18, 19]. Models 2 and 3 describe point defects in an averaged structure. The excess of Nb atoms replaces Li atoms at Li sites. Models 2 and 3 differ in the way of achieving charge neutrality. In model 2 the occupation of the Nb

sublattice remains 100% and every four vacant Li sites (charge of -4) are statistically accompanied by one Li site occupied by a Nb atom (difference charge of $+4$ at this site). In model 3 the excessive charge of five Nb atoms on Li sites (charge $+20$) is compensated by four vacant Nb sites (charge -20), as shown in Fig. 1. Thus, in model 2 charge neutrality is achieved by Li vacancies, whereas in model 3 the charge neutrality is supposed to be realized by Nb vacancies. One can see from the formula in Table 1 that in model 2 about 1% of Nb atoms are located on "wrong" sites and model 3 requires about 5% of "wrong" positioned Nb atoms. NMR measurements of ^{93}Nb [5, 14] indicate different chemical surroundings (coordination) of about 5% of all Nb atoms in congruent LN, supporting defect model 3. This model has also been supported by a later X-ray structure analysis [4]. Combined Rietveld diffraction analysis with both X-rays and neutrons (time of flight) recently showed a fully occupied Nb sublattice [6, 7], strongly supporting defect model 2. In Fig. 1, the cationic sequences along c_{hex} for models 2 and 3, as well as for the idealized LN structure and Ilmenite-type structure, which can also be realised in LN [20], are shown. The interpretation of models 2 and 3 on an atomic scale shows that Nb atoms at Li sites in models 2 and 3 necessarily give a cationic sequence parallel to the axis c_{hex} of two Nb atoms in neighbouring octahedra (see Fig. 1). Model 3 was proposed by Donnerberg *et al.* [21] to consist of two different sequences (a) and (b), where the sequence (a) can be interpreted as a disordered Ilmenite-type structure. Model 2 also consists of two different cationic sequences (a) and (b). It was predicted by Lerner *et al.* [15] and confirmed by Donnerberg *et al.* [21] on the basis of computer calculation of defect energy minima.

Thus, the Li vacancy defect model is supported by computer simulations [21] and, as mentioned above, by diffraction studies [6, 7], contradicting the results of NMR [5, 14] and a structure report [4]. To clarify this contradiction a new NMR study was performed.

EXPERIMENTAL

All the measurements were made on a Fourier Transform Bruker MSL 300 Solid State NMR spectrometer. Thus, the Larmor frequencies for ^{7}Li and ^{93}Nb were 116.6 and 73.5 MHz, respectively. LN was measured either as a finely ground powder or as single crystals with defined direction of the c-axis. For the MAS spectra, the powdered samples were packed in 7 mm ZrO_2 rotors and spun with rotational frequencies up to 4 kHz. Single crystals were measured in the form of manufactured plates (dimensions: 5 mm × 0.5 mm × 10 mm) in 5 mm (^{7}Li) and 10 mm (^{93}Nb) solenoidal coils. The piezoelectric response [22] of the single crystals could be suppressed efficiently by wrapping them with adhesive tape. Therefore, a simple single pulse sequence with a short 90° pulse (2 μs) and a dead time delay of 8 μs could be used. Further details are given with the respective spectra.

SOLID STATE NMR OF LITHIUM NIOBATE

LN offers three different nuclei that can in principle be measured by NMR spectroscopy. However, quadrupolar ^{17}O with its low natural abundance is still beyond reach for solid state NMR of samples that are not enriched. ^{7}Li and ^{93}Nb, on the other hand, have high natural abundances (92.6% and 100%), but are also quadrupolar nuclei, with $I = \frac{3}{2}$ and $\frac{9}{2}$, respectively. Therefore, the NMR signals are often very broad and even asymmetric due to quadrupolar interactions with the electric field gradient. Several strategies have been developed recently in order to decrease the line width of quadrupolar nuclei: magic angle spinning (MAS) [23], dynamic angle spinning (DAS) [24], double orientation rotation (DOR) [25] and using as high a permanent magnetic field as possible. Additionally, the information content can be increased by two-dimensional nutational NMR [26]. Whereas DAS and DOR are still technically demanding, MAS and high magnetic fields are readily available today. It is this approach that has been chosen here, using a magnetic field strength of 7.05 Tesla.

^{7}Li NMR SPECTROSCOPY

Early ^{7}Li studies have already been done by Halstead [8], who investigated atomic motions in LN single crystals. At the very low magnetic field strength available then (0.75 Tesla, corresponding to a Larmor frequency of 8 MHz), the minimum value for the line width at room temperature was about 9 kHz. A later

Table 1.

Model no.	Parametric formula	Kröger–Vink notation	Chemical formula (48.4% Li_2O)	Authors
1	$Li_{1-2x}NbO_{3-x}$	$2\,V_{Li}V_O$	$Li_{0.9371}NbO_{2.9686}$	Bollmann [17]
2	$[Li_{1-5x}Nb_x]NbO_3$	$Nb_{Li}4V_{Li}$	$[Li_{0.947}Nb_{0.0106}]NbO_3$	Lerner [15]
3	$[Li_{1-5x}Nb_{5x}]Nb_{1-4x}O_3$	$5Nb_{Li}4V_{Nb}$	$[Li_{0.947}Nb_{0.053}]Nb_{0.9576}O_3$	Abrahams [4]

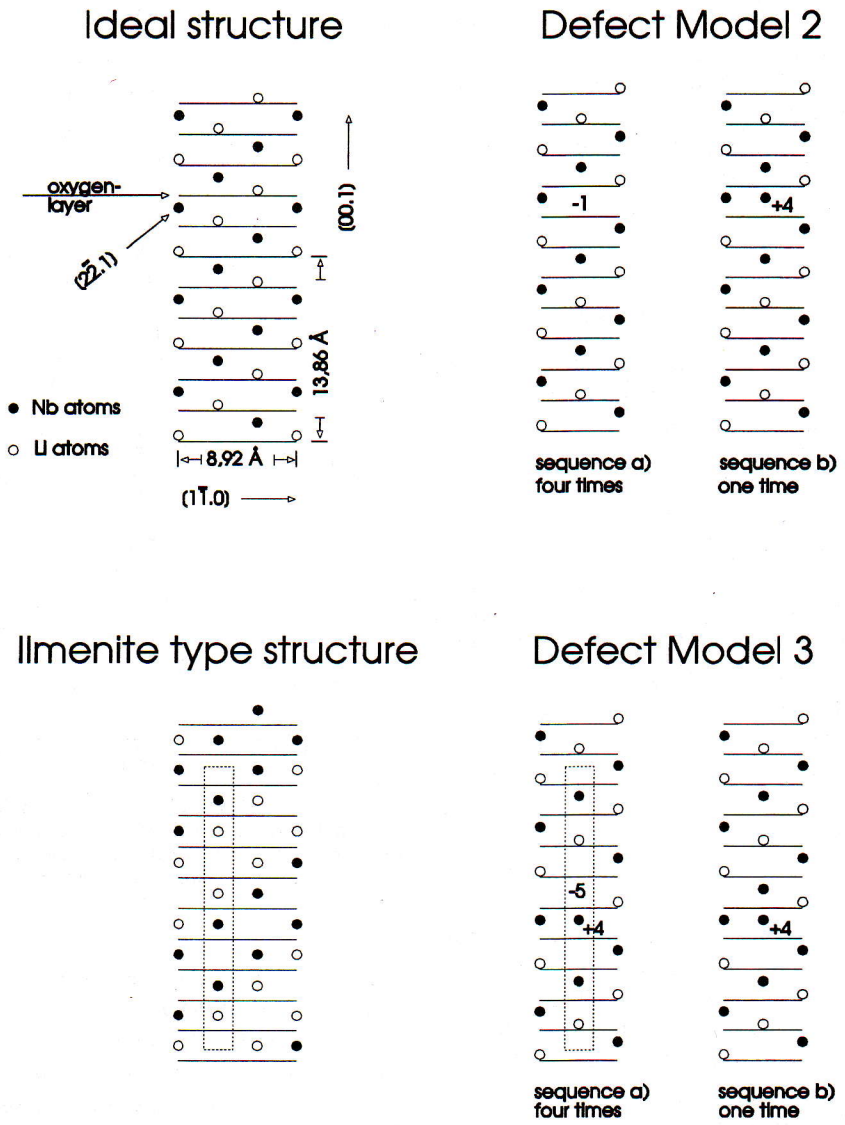

Fig. 1. Cation arrangements of ideal LN, idealized Ilmenite-type LN, defect model 2 and defect model 3 are drawn in a cut parallel to the plane (11$\bar{2}$0). The formal charges of the "wrong" occupied oxygen octahedra in defect model 2 and defect model 3 are declared. The relationship between the cation sequences in the Ilmenite-type structure and defect model 3 is marked by the dashed rectangle.

study of LN powder samples [9] did not make a very reliable impression, since the spectra were grossly distorted, maybe due to clipped FIDs or piezoelectric ringing [22].

If one considers only the oxygen coordination of the Li atoms, there is no reason for a second NMR resonance caused by the defect structure given, because all Li atoms occupy their regular lattice site. The situation changes if the effect of vacancies and Nb atoms positioned on Li sites caused by the defect structure is taken into account. In this case, in model 2 as well as in model 3 the perfect sequence of the Li atoms along (2$\bar{2}$.1) is disturbed by vacancies and Nb atoms, respectively (see Fig. 1), which may give rise to a second ^{7}Li resonance. While a single crystal measurement of ^{7}Li could not diminish the line width found earlier [8], rotating a powder sample about the magic angle with a rotational frequency of 4000 Hz gave a residual line width of only 0.6 kHz (see Fig. 2). This means an improvement of more than an order of magnitude as compared to earlier results. Thus, the quadrupolar interactions could efficiently be reduced by MAS alone in this case. The overall appearance of the single signal is completely symmetric, all rotational sidebands [23] with the same distance to the central line have equal height; the isotropic line does not show any shoulder, which additionally

makes the assumption that another signal should be hidden underneath unlikely.

So, the ^{7}Li NMR spectrum supports neither defect model 2 nor defect model 3, although the impact of the surroundings of the ^{7}Li nucleus on its chemical shift is not known and the overall chemical shift range [27] is about three times the observed residual line width.

^{93}Nb NMR SPECTROSCOPY

As compared to ^{7}Li, ^{93}Nb has a much greater chemical shift range of several thousand ppm [27] and therefore became the object of further investigation. ^{93}Nb NMR spectroscopy always uses the most intense central $-1/2 \rightarrow +1/2$ transition.

Early NMR studies of ^{93}Nb in LN have already been performed in 1967 by Peterson and Bridenbaugh [10], who determined the quadrupolar coupling constant (22.02 MHz). Later, he used ^{93}Nb NMR spectroscopy of powder samples as a probe of stoichiometry in LN [11]. Finally, an attempt was made by Peterson and Carnevale [5] to distinguish between the defect models 2 and 3 (Fig. 1) for Li-deficient materials by single crystal ^{93}Nb NMR measurements.

In principle, due to the large chemical shift range of ^{93}Nb (see below and ref [27]), different signals for Nb nuclei in different chemical surroundings are expected. Considering only the oxygen surroundings, both defect models could theoretically give more than one ^{93}Nb resonance. Besides the prominent ^{93}Nb NMR signal of the regular lattice {o Nb Li o}, model 2 requires one more signal with about 1% the intensity that stems from Nb atoms at Li sites {o Nb Nb o}. According to model 3, one more signal with a relative intensity of about 5% could in principle be expected from Nb atoms occupying larger Li octahedra {o o Nb o} and {o Nb Nb o} (see Fig. 1).

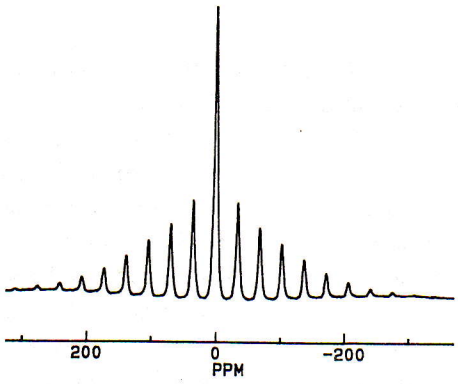

Fig. 2. 116.6 MHz ^{7}Li MAS spectrum of powdered LN. Single pulse excitation with a 90° pulse width of 4 μs and a deadtime delay of 5 μs; 2000 transients were accumulated at a rotational frequency of 4 kHz.

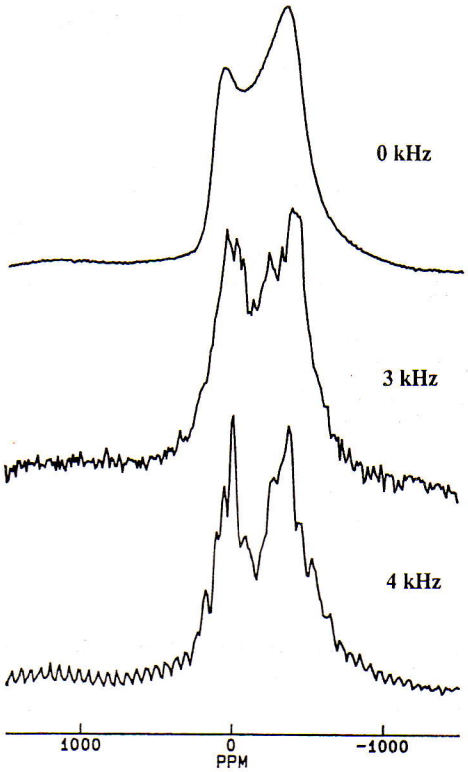

Fig. 3. 73.5 MHz ^{93}Nb MAS spectra of powdered LN at the rotational frequencies indicated. Single pulse excitation with a 90° pulse width of 2 μs and a deadtime delay of 5 μs. Pulse repetition rate 500 ms.

The situation will become more complicated if the effect of Nb atoms and vacancies positioned on Li sites is examined on Nb atoms in regular lattice sites. Model 3 was strongly favoured by Peterson and Carnevale [5], but later a careful measurement combined with elaborate simulation studies showed that the interpretation of the ^{93}Nb NMR spectra is less straightforward than thought previously [12]. The conclusions drawn recently by Hu *et al.* [14] are dubious, because they are based mainly on ^{93}Nb NMR powder spectra of very bad signal-to-noise ratio and the dubious second signal might just be a part of the asymmetric wideline signal.

In contrast to the ^{7}Li NMR measurements, MAS did not improve the ^{93}Nb NMR spectra substantially. The second order quadrupolar interactions are too great to be removed by MAS alone. Even at a rotational frequency of 4000 Hz the isotropic lines cannot be resolved (Fig. 3). At the same time the typical changes of the appearance of the signal with spinning frequency are obvious. Since the detection of a resonance of low intensity was impossible in the complex MAS spectra, a single crystal study analogous to the one performed by Peterson *et al.* [12] was undertaken. The single crystals were rotated

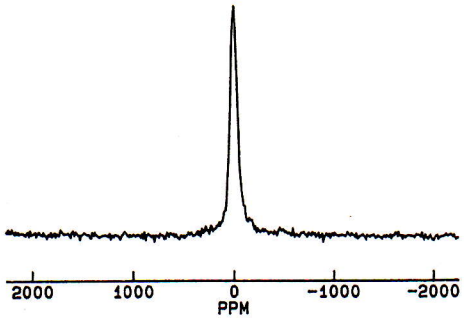

Fig. 4. 73.5 MHz ^{93}Nb NMR spectrum of an LN single crystal with the c-axis aligned to the external magnetic field. Single pulse excitation with a 90° pulse width of 2 μs and a deadtime delay of 8 μs; 14,000 scans were accumulated with a pulse repetition rate of 200 ms.

about the axis c_{hex} in 5° steps. However, none of these crystal orientations yielded a second signal within the spectra or even a shoulder. The minimum line width at our magnetic field of 7.05 Tesla was 5 kHz (see Fig. 4) and the maximum one 22 kHz; the total spanned chemical shift range was about 1000 ppm. Since a second resonance with a deviant electric field gradient of small asymmetry parameter with about 5% intensity as compared to the main signal should have been detected with our procedure, there are two explanations that can be given.

(1) The second resonance found earlier was just an artefact due to the low magnetic field strengths available then. This—together with recent X-ray results [6, 7]—would strongly favour defect model 2, which requires a second resonance in the 1% intensity region that cannot possibly be detected in the spectra of strongly quadrupolar nuclei.

(2) The sought after second resonance behaves like the main signal and is always hidden under the latter. In this case NMR spectroscopy would not be the right choice of probe to distinguish between defect models 2 and 3.

Finally, a two-dimensional nutational NMR spectrum of an LN single crystal with the axis c_{hex} aligned to the direction of the magnetic field, in analogy to the one performed by Man *et al.* with LN powder [13], was undertaken. However, even in the two-dimensional nutational NMR spectrum, no second resonance with a different nutational frequency could be detected.

REFERENCES

1. Abrahams S. C., Reddy J. M. and Bernstein J. L., *J. Phys. Chem. Solids* **27,** 997 (1966).
2. Megaw H., *Acta Cryst.* **A24,** 583 (1968).
3. Born E., Grabmayer B. C., Hofmann K. and Willibald-Riha E., European Patent 0417132131.
4. Abrahams S. C. and Marsh P., *Acta Cryst.* **B42,** 61 (1986).
5. Peterson G. E. and Carnevale A., *J. Chem. Phys.* **56,** 4848 (1972).
6. Zotov N., Boysen H., Frey F., Metzger Th. and Born E., *J. Phys. Chem. Solids* **55,** 145 (1994).
7. Iyi N., Kitamura K., Izumi F., Yamamoto J. K., Hayashi T., Asano H. and Kimura S., *J. Solid State Chem.* **101,** 340 (1992).
8. Halstead T. K., *J. Chem. Phys.* **53,** 3427 (1970).
9. Baiqin L., Yening W. and Ziran X., *J. Phys. C: Solid State Phys.* **21,** L251 (1988).
10. Peterson G. E. and Bridenbaugh P. M., *J. Chem. Phys.* **48,** 3402 (1968).
11. Peterson G. E. and Carruthers J. R., *J. Solid State Chem.* **1,** 98 (1969).
12. Douglass D. C., Peterson G. E. and McBrierty V. J., *Phys. Rev.* **B40,** 10694 (1989).
13. Man P. P., Theveneau H. and Papon P., *J. Magn. Reson.* **64,** 271 (1985).
14. Hu L. J., Chang Y. H., Yang S. J., Hu M. L. and Tse W. S., *Mod. Phys. Lett.* **B5,** 789 (1991).
15. Lerner P., Legras C. and Dumas J. P., *J. Cryst. Growth* **3,4,** 231 (1968).
16. Nassau K. and Lines M. E., *J. Appl. Phys.* **41,** 533 (1970).
17. Bollmann W., *Cryst. Res. Technol.* **18,** 9, 1147 (1983).
18. Kovacs L. and Polgar K., *Cryst. Res. Technol.* **21,** K101 (1986).
19. Holmes R. J. and Minford W. J., *Ferroelectrics* **75,** 63 (1987).
20. Kumada N., Ozawa N., Muto F. and Kinomura N., *J. Solid State Chem.* **57,** 267 (1985).
21. Donnerberg H. J., Tomlinson S. M. and Catlow C. R. A., *J. Phys. Chem. Solids* **52,** 203 (1991).
22. Hughes D. G. and Pandey L., *J. Magn. Reson.* **56,** 428 (1984).
23. Herzfeld J. and Berger A. E., *J. Chem. Phys.* **73,** 6021 (1980).
24. Mueller K. T., Wooten E., W. and Pines A., *J. Magn. Reson.* **92,** 620 (1991).
25. Samoson A. and Lippmaa E., *J. Magn. Reson.* **84,** 410 (1989).
26. Samoson A. and Lippmaa E., *Phys. Rev.* **B28,** 6567 (1983).
27. *Multinuclear NMR* (Edited by J. Mason), Plenum Press, New York (1987).